Dentomaxillofacial Radiology (2018) 47, 20180021

birpublications.org/dmfr

RESEARCH ARTICLE

Magnitude of cone beam CT image artifacts related to zirconium and titanium implants: impact on image quality

[1]Rocharles C Fontenele, [1]Eduarda HL Nascimento, [1]Taruska V Vasconcelos, [2]Marcel Noujeim and [1]Deborah Q Freitas

[1]Department of Oral Diagnosis, Division of Oral Radiology, Piracicaba Dental School, University of Campinas, Piracicaba, São Paulo, Brazil; [2]Department of Comprehensive Dentistry, Division of Oral and Maxillofacial Radiology, University of Texas Health Science Center, San Antonio, TX, USA

Objectives: To evaluate the magnitude of artifacts related to titanium and zirconium implants at different distances and angulations and their impact on cone beam CT(CBCT) image quality.
Methods: CBCT images were obtained before and after the insertion of titanium and zirconium implants in a mandible on different CBCT units: Picasso Trio, ProMax 3D and 3D Accuitomo 80. Artifact was assessed by measuring the standard deviation (SD) of gray values and contrast-to-noise ratio (CNR) of 11 regions of interest (ROIs) at different distances (1.5 cm, 2.5 cm and 3.5 cm) and angulations (65°, 90°, 115° and 140°) from implant region.
Results: For titanium images, SD values did not differ from those of images without implant in all ROIs; however, some effect occurred in Picasso images as higher values were observed in ROIs closer to the implant ($p < 0.05$). Zirconium images showed higher SD values than the others in some ROIs for Picasso and ProMax ($p < 0.05$). In ProMax, the difference was observed even in the farthest ROIs from the implant. CNR values were not influenced by the ROI in Picasso, but presented lower values in ROIs closer to the zirconium implant for ProMax and Accuitomo.
Conclusions: The quantity and magnitude of artifacts in CBCT are influenced by the type of implant and CBCT unit. Although they are more pronounced in regions closer to the implant and located at 90° in relation to the mandibular long axis, they can reach as far as 3.5 cm from the artifact-generator object.
Dentomaxillofacial Radiology (2018) **47**, 20180021. doi: 10.1259/dmfr.20180021

Cite this article as: Fontenele RC, Nascimento EHL, Vasconcelos TV, Noujeim M, Freitas DQ. Magnitude of cone beam CT image artifacts related to zirconium and titanium implants: impact on image quality. *Dentomaxillofac Radiol* 2018; **47**: 20180021.

Keywords: cone beam CT; metal artifacts; titanium; zirconium

Introduction

Accurate pre-operative surgical planning and post-operative evaluation are important steps for a successful dental implant rehabilitation. Cone beam CT (CBCT) is recommended by several oral radiology guidelines as a pre-operative examination for dental implants planning,[1,2] whereas other guidelines recommend its use only in situations where there is clinical doubt about bone shape or anatomical borders,[3] which happens in many cases. Therefore, this examination is widely used in Implantology in pre-operative evaluation. In contrast, CBCT is not a part of a routine protocol for implant post-operative examinations due to limitations inherent to the image formation process, which leads to artifacts formation and may hinder or prevent the proper diagnosis and/or analysis of the peri-implant site.[4–6]

Artifacts in CBCT images represent structures visualized after data reconstruction, that do not correspond to real features of the evaluated object.[5,7] Their

Correspondence to: Dr Deborah Q Freitas, E-mail: deborah@fop.unicamp.br; deborahq@unicamp.br
Received 16 January 2018; revised 22 March 2018; accepted 16 April 2018

origin is related to the differences between real physical characteristics from the objects and its attenuation coefficient which will be received by the detector, besides limitations from the CBCT unit itself, such as mathematical algorithm particularities in the retroprojection used for the image reconstruction process. Moreover, the composition and positioning of objects within the field of view (FOV) may interfere significantly in this process.[6–8]

Among the several artifact types found in CBCT images, there are those caused by the presence of high atomic number and density structures, such as dental implant constitutive materials.[5–7] One of the main factors responsible for image degradation from this type of artifact is the beam-hardening phenomenon. High-density structures act as a filter, increasing the average energy of the radiation beam reaching the detector. This results in the production of an error in the data reconstruction that results in the deterioration of image quality in the vicinity of these objects, represented in the image as linear structures, bands and shadows organized along the projection.[5,7,9]

In addition to beam hardening, the noise and dispersion effects also have an influence on the image quality.[10] When associated, they tend to cause the formation of artifacts such as cupping, streaks and dark bands between dense objects or streaks at sharp edges with high contrast to neighboring structures.[11,12] This occurs because beam hardening and the noise effect induces an excessive gray values variation close to high- density objects, such as dental implant, resulting in drastically decreased values, producing images with reduced contrast and compromising diagnosis by obscuring nearby structures.[13]

Since the implants commercialized nowadays are made of high-density materials, such as titanium and zirconium, the presence of artifacts in their CBCT image is inevitable. Their production and effect around the artifact-generator object have been studied in previous years.[5,6,9,13–15] However, it seems there are no studies showing how far the artifact production could reach or which type of dental implant has greater advantages when evaluating its magnitude and, thereafter, the impact on CBCT image quality. Although previous studies have evaluated metal artifacts in CBCT images, the majority of them have been qualitative ones and few studies have quantitatively compared CBCT machines.[9,16] This factor is relevant since the different machines available in the market may present significant technical differences, which interfere with their image quality and artifact formation.[9,17] Additionally, besides the CBCT examination is not considered the first choice image for post-implant evaluation,[1] dental implants included in the scanned region in examinations performed for other purposes can compromise the image quality. Hence, investigations about the magnitude from artifacts produced by different types of dental implants in different CBCT machines are still needed in the literature.

Thus, the purpose of this study was to evaluate the magnitude of artifacts related to titanium and zirconium implants and its impact on CBCT image quality using three CBCT units.

Methods and materials

This study design was approved by the local institutional research Review Board (protocol #2.163.038).

Sample preparation

The alveolar bone was prepared for dental implant placement in the region of the tooth 46 in two dry human mandibles. An epoxy resin-based tissue substitute (ERBS) block (9 × 4 × 4 mm) was fixed on the surface of the buccal cortical plate of each mandible at the middle level of the implant cavity to serve as a reference to select the axial images in which the evaluations would be performed. One axial slice image was chosen, being a first image in which the ERBS block was visualized in the coronal-apical orientation. An additional ERBS block (18 × 10 × 7 mm) was inserted in the anterior buccal cortical plate of the mandible aligned to its middle line and also at the middle level of the implant in height to serve as a control area. This was decided because the artifacts seemed to be pronounced in the ERBS block positioned closed to the implant in the pilot tests, which would impair its use as a control area.

4 × 11 mm titanium (Titamax, Neodent, Brazil) and zirconium oxide (Z-Look3, Z-systems, Switzerland) implants were alternately inserted in the mandibles.

Image acquisition

Picasso Trio 3D unit (Vatech, Hwaseong, South Korea), ProMax 3D (Planmeca Oy, Helsinki, Finland) and 3D Accuitomo 80 (Morita, Kyoto, Japan) units were used to scan the mandibles. The acquisition protocol and technical aspects of CBCT units are shown in Table 1. The parameters selected are in accordance with the manufacturer's recommendations of each CBCT unit as the optimal exposure setting for average adult patient.

Each mandible was placed inside a cylindrical plastic container (16 cm diameter) filled with water for soft tissue simulation[5,18] and kept in position by the help of an impression material. The container was placed in the

Table 1 Exposure protocols and technical aspects related to CBCT units

CBCT unit	*kVp*	*mA*	*FOV (cm)*	*Voxel size*	*Exposure time (s)*	*Frames*
Picasso Trio	80	5	8 × 5	0.2	24	720
ProMax 3D	80	5	8 × 5	0.2	12	251
3D Accuitomo 80	80	5	8 × 8	0.2	17.5	640

CBCT, cone beam CT; FOV, field of view.

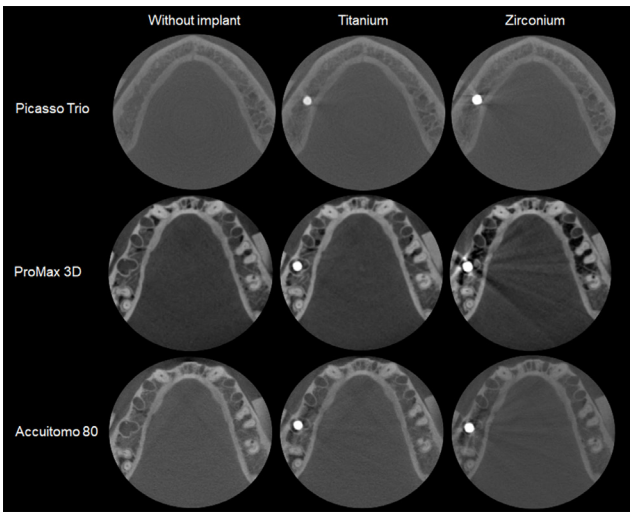

Figure 1 Examples of cropped axial views of "without implant", "titanium" and "zirconium" groups acquired in units studied.

center of the FOV and the images were acquired before and after insertion of the implants to generate three sets of images: a control set (without implant), a titanium set and a zirconium set. Figure 1 shows examples of axial views of groups and units studied. For each condition (without implant, with titanium or zirconium implant), three examinations were acquired to assess the study reproducibility, totaling 27 CBCT scans (3 experimental groups × 3 CBCT machines × 3 acquisitions).

Image analysis

To standardize the image selection in the proprietary viewing software of each CBCT unit, the axial slice corresponding to the middle level of the implant height was selected using the ERBS block as reference. Then, the axial slices were exported to ImageJ software (National Institutes of Health, Maryland, MD) to obtain the mean and standard deviation (SD) of gray values in 11 regions of interest (ROIs). The analyses were performed in 16-bits images. For standardizing the ROIs positions and covering the main region of artifact production, a line was determined in the center of implant image following the long axis of the mandible body; next, a line perpendicular to the first one (90°) was determined; last, three lines (two anterior at 115 and 140° and one posterior at 65°) 25° distant from each other were drawn. After, from the center of the implant, three semi-circles were drawn with radii of 1.5, 2.5 and 3.5 cm. Finally, 11 square ROIs of 2.8 × 2.8 mm were established on the intersection of circles and lines (Figure 2). The macro function of Image J software was used to determine and analyze the same area in all images. Three different macros with the same pattern were recorded: one for each set of images of each machine.

Subsequently, an additional ROI with same size was determined on the ERBS block (Figure 2c) and served as a control area to enable the contrast-to-noise ratio (CNR) calculation, according to this formula[12]:

$$CNR = \frac{|Mean_{Implant} - Mean_{Control}|}{\sqrt{SD^2_{Implant} + SD^2_{Control}}}$$

Statistical analysis

The analyses were performed using SPSS software v. 24.0 (IBM Corp., Armonk, NY) with a significant p-value < 0.05.

The SD and CNR were compared by analysis of variance (ANOVA two-way) with post-hoc Tukey test, in order to test the effects of the region and implants. The ANOVA was conducted independently for each machine; so their results were not matched. The null hypothesis was that the regions or implant presence did not have an influence on SD or CNR.

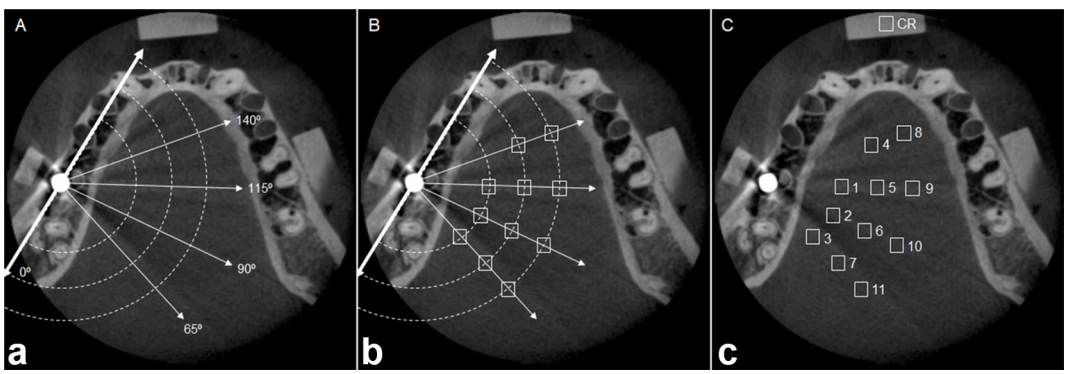

Figure 2 Determination of the ROIs to evaluate the magnitude of artifacts. (a) One line was determined in the center of implant image following the long axis of the mandible body. Four additional lines at angles of 65°, 90°, 115° and 140° in relation to the first were drawn passing through the central region of the implant. From this centered point, three semi-circles were drawn with radii of 1.5, 2.5 and 3.5 cm. (b) On the intersection of circles and lines, 11 square ROIs of 2.8 × 2.8 mm were established over three distance levels and four angles in relation to the implant region. (c) Final location of the ROIs and the additional CR were placed on the ERBS block. CR, control ROI; ERBS, resin-based tissue substitute; ROIs, regions of interest.

Results

Standard deviation

Table 2 summarizes the results for the SD of the ROIs evaluated in the different groups and scanners tested. Regarding the effect of the presence of the implant, there were no differences between the control and titanium groups for all ROIs and CBCT units ($p > 0.05$). In contrast, zirconium group had higher SD values ($p < 0.05$), especially closer to the implant for Picasso Trio (ROI 1), in several distances but at 90° from the implant for ProMax (ROIs 1–3, 5–6, 9–10), and in one isolated ROI for Accuitomo (ROI 5).

Regarding the effect of the region, the control group showed no statistical differences among all evaluated ROIs for the three CBCT units ($p > 0.05$). For the titanium group, some effect was observed in images of Picasso since, although there was no difference from control group in each region, different values were found between the ROIs, which showed in general higher SD values in the regions closer to the implant. For the other CBCT units, there were no differences between the ROIs studied. For zirconium groups, there were significant differences between the zones of artifact production in the three CBCT units tested. In general, farther the region from the implant, lower was the SD, except for Accuitomo, ROI 5.

Contrast-to-noise-ratio

The CNR values according to different groups and scanners tested are shown in Table 3. Regarding the implant effect, the control and titanium groups showed no differences for the Picasso and ProMax ($p > 0.05$), but both had higher CNR than the zirconium group ($p < 0.05$). For the Accuitomo, there was no effect of implants on the CNR ($p < 0.05$).

The CNR was not influenced by ROI in the control and titanium groups for the three CBCT units ($p > 0.05$), while the zirconium groups had variable results depending on the scanner. For Picasso, the CNR of the zirconium group was also not influenced by ROI ($p > 0.05$). On the other hand, the zirconium groups of the ProMax and Accuitomo showed lower CNR values in the regions closer to the implant and in the central zone of artifacts production (notably in the ROIs 1 and 5).

Discussion

The expression of artifacts in the regions close to high-density materials on CBCT images has already been previously reported.[5,8] Nonetheless, the present study is the first to evaluate the magnitude, that is, the intensity of the artifacts at different distances from their forming region, using three scanners and different dental implants for this purpose. In addition to the evaluation of artifacts related to titanium implants, which

Table 2 Mean of SD values of the ROIs according to the groups and CBCT units evaluated

	Picasso Trio—Mean (SD)			*ProMax 3D—Mean (SD)*			*3D Accuitomo 80—Mean (SD)*		
ROI	*Control*	*Titanium*	*Zirconium*	*Control*	*Titanium*	*Zirconium*	*Control*	*Titanium*	*Zirconium*
1	63.07 (9.53) Aa	69.12 (10.44) Ab	86.58 (19.81) Bc	58.97 (7.63) Aa	65.58 (4.16) Aa	111.05 (7.00) Bd	119.47 (21.12) Aa	115.63 (27.30) Aa	135.32 (15.30) Ab
2	56.21 (2.41) Aa	53.73 (2.45) Aab	61.05 (2.47) Aab	55.47 (9.69) Aa	54.09 (5.52) Aa	98.08 (6.07) Bcd	102.82 (7.99) Aa	101.47 (19.57) Aa	128.43 (4.97) Aab
3	54.90 (5.17) Aa	62.28 (9.13) Aab	67.70 (6.06) Ab	61.36 (8.56) Aa	61.54 (3.42) Aa	85.81 (2.76) Bbc	111.76 (21.22) Aa	105.71 (9.98) Aa	132.04 (11.88) Ab
4	54.90 (5.17) Aa	62.28 (9.13) Aab	67.70 (6.06) Ab	63.93 (12.86) Aa	60.94 (7.93) Aa	72.62 (5.38) Aab	104.30 (2.20) Aa	112.20 (8.86) Aa	105.08 (17.56) Aab
5	47.15 (2.78) Aa	50.69 (2.02) Aa	49.32 (3.80) Aa	49.44 (10.25) Aa	60.38 (11.65) Aa	97.74 (17.67) Bcd	128.75 (10.32) Aa	136.37 (27.53) Aa	179.32 (25.92) Bc
6	50.38 (5.44) Aa	48.19 (4.26) Aa	52.71 (3.33) Aab	54.22 (13.09) Aa	53.78 (7.02) Aa	72.44 (6.10) Bab	103.20 (15.91) Aa	114.36 (2.03) Aa	102.24 (6.09)Aab
7	58.34 (13.62) Aa	51.81 (6.71) Aab	59.67 (3.06) Aab	59.86 (8.47) Aa	52.61 (5.51) Aa	67.88 (7.45) Aab	97.29 (23.40) Aa	121.70 (10.22) Aa	106.89 (17.91) Aab
8	65.09 (3.46) Aa	62.38 (6.02) Aab	62.38 (8.13) Aab	57.90 (1.53) Aa	58.38 (7.95) Aa	60.81 (2.06) Aa	111.33 (8.16) Aa	102.08 (15.58) Aa	94.13 (0.70) Aa
9	54.43 (2.22) Aa	61.44 (3.12) Aab	61.60 (4.70) Aab	58.05 (9.36) Aa	60.67 (7.43) Aa	80.93 (3.36) Babc	97.71 (18.51) Aa	107.51 (17.68) Aa	103.47 (9.54) Aab
10	49.21 (3.73) Aa	46.32 (2.97) Aa	54.05 (4.40) Aab	54.94 (3.74) Aa	58.21 (5.55) Aa	81.60 (4.25) Babc	88.01 (19.66) Aa	102.36 (6.44) Aa	104.86 (9.90) Aab
11	58.35 (1.68) Aa	57.67 (6.22) Aab	57.20 (5.40) Aab	46.19 (7.36) Aa	60.69 (8.65) Aa	60.53 (4.10) Aa	93.51 (8.84) Aa	98.10 (7.36) Aa	104.91 (9.03) Aab

CBCT, cone beam CT; ROI, region of interest; SD, standard deviation.
Different uppercase letters indicate statistical difference between control, titanium and zirconium groups within each CBCT unit; and different lowercase letters indicate statistical difference between ROIs within each group, according to ANOVA two-way.

Table 3 Mean of CNR values of the ROIs according to groups and CBCT units evaluated

	Picasso Trio—Mean (SD)			*ProMax 3D—Mean (SD)*			*3D Accuitomo 80—Mean (SD)*		
ROI	*Control*	*Titanium*	*Zirconium*	*Control*	*Titanium*	***Zirconium***	*Control*	*Titanium*	*Zirconium*
1	9.61 (1.24) Aa	9.41 (0.90) Aa	8.41 (0.64) Ba	14.52 (2.22) Aa	12.63 (1.16) Aa	8.47 (0.74) Bb	4.12 (0.26) Aa	4.11 (0.50) Aa	3.56 (0.32) Abc
2	10.12 (1.25) Aa	10.31 (0.76) Aa	9.66 (1.32) Ba	14.66 (2.68) Aa	14.89 (0.84) Aa	10.60 (0.08) Bab	4.28 (0.16) Aa	4.61 (0.54) Aa	4.42 (0.20) Aa
3	10.11 (1.27) Aa	9.29 (1.05) Aa	8.31 (1.20) Ba	14.07 (0.68) Aa	13.88 (0.71) Aa	9.51 (0.27) Bab	4.12 (0.41) Aa	4.15 (0.33) Aa	3.81 (0.15) Aabc
4	10.11 (1.27) Aa	9.29 (1.05) Aa	8.31 (1.20) Ba	13.31 (1.23) ABa	14.31 (0.84) Aa	11.01 (1.09)Bab	4.43 (0.18) Aa	4.13 (0.26) Aa	4.59 (0.63) Aa
5	10.30 (1.32) Aa	10.11 (0.75) Aa	9.64 (1.30) Ba	16.04 (3.27) Aa	13.58 (1.30) Aa	8.92 (1.64) Bb	3.98 (0.06) Aa	3.60 (0.53) Aa	2.85 (0.26) Ac
6	10.52 (1.60) Aa	10.45 (0.96) Aa	9.78 (1.38) Ba	14.87 (0.77) Aa	15.40 (0.84) Aa	11.90 (0.14) Bab	4.44 (0.46) Aa	4.07 (0.08) Aa	4.64 (0.16) Aa
7	10.55 (1.20) Aa	10.56 (0.81) Aa	9.61 (1.32) Ba	14.35 (1.29) ABa	15.37 (1.31) Aa	12.01 (0.06) Bab	4.66 (0.78) Aa	3.95 (0.31) Aa	4.61 (0.43) Aa
8	9.05 (0.84) Aa	8.88 (0.91) Aa	8.40 (1.45) Ba	12.84 (1.23) Aa	13.82 (1.39) Aa	11.49 (0.66) Aab	3.98 (0.22) Aa	4.13 (0.35) Aa	4.45 (0.18) Aab
9	10.45 (1.35) Aa	10.04 (0.79) Aa	9.52 (1.22) Ba	15.17 (2.48) Aa	13.85 (1.07) Aa	10.38 (0.82) Bab	4.69 (0.67) Aa	4.20 (0.46) Aa	4.31 (0.49) Aab
10	10.76 (1.11) Aa	10.78 (0.82) Aa	9.92 (1.20) Ba	15.07 (2.06) Aa	14.49 (0.59) Aa	11.00 (1.01) Bab	4.86 (0.60) Aa	4.47 (0.05) Aa	4.69 (0.27) Aa
11	10.51 (1.15) Aa	10.38 (0.83) Aa	9.76 (1.40) Ba	16.38 (2.36) Aa	14.58 (0.68) ABa	13.14 (1.33) Ba	4.75 (0.25) Aa	4.45 (0.33) Aa	4.61 (0.22) Aa

CBCT, cone beam CT; CNR, contrast-to-noise ratio; ROI, regions of interest; SD, standard deviation.
Different uppercase letters indicate statistical difference between control, titanium and zirconium groups within each CBCT unit; and different lowercase letters indicate statistical difference between ROIs within each group, according to ANOVA two-way.

are further investigated in the literature because of their longer use in Implantology, the present study also evaluated the magnitude of artifacts related to zirconium implants. This material has been increasingly used for presenting high biocompatibility, good osseointegration properties, fair success rates and for being metal free, which gives it high aesthetic results.[5] As results, we found that different types of high-density materials and CBCT units present different behaviors regarding expression and magnitude of artifacts in CBCT images.

The use of human mandibles placed in cylindrical plastic container filled with water for simulation of attenuation and dispersion of X-ray beams through soft tissues is important for reproduction of an *in vivo* situation.[5] Different mandibles have been used as phantom for the different units in this study. Although we recognize that this is not the ideal study condition, since some possible interference on the raw data could be present, but was not investigated, all the images acquired in each CBCT unit were obtained using a single mandible and the same dental implants, positioned in a standardized region. In addition, the SD and CNR values were not directly compared between the CBCT units. Therefore, we believe the use of two mandibles did not affect the overall results and conclusions of the study.

The acquisition protocol used for each CBCT unit was selected according to the manufacturer's recommendations as the optimal exposure setting for average adult patient, although it is known that the exposure parameters should ideally consider both patient features and indication related to specific diagnostic tasks in order to obtain dose reduction at a satisfactory image quality.[19,20] The main technical differences between the CBCT units evaluated were the number of basis images and time of exposure. In a same CBCT unit, the higher the number of basis images, the better image quality is expected, because there are more data to reconstruct the images. Likewise, it has been shown that increases in kVp and mAs are related to a decrease in artifact production in CBCT images.[5,9,14] In the present study, CBCT units were not directly compared because other factors are also related to image formation and artifacts expression, such as mathematical algorithms for image reconstruction and image receptor technology. However, according to our results, it seems that examinations with lower number of basis images produce more artifacts.

As in previous studies,[5,9,16,21] the objective evaluation of artifact production in CBCT images was performed by calculating the SD of gray values and CNR. SD values allow a general estimation of darkening and brightening extension caused by high-density materials as measure by the variation of gray values. So higher SD value or higher variation indicates higher artifact production. The evaluation of the magnitude of artifacts was done through the comparison between values obtained in the regions closer to the implants and in the more distant regions, in different angulations. On the other hand, the CNR evaluation was made after the

selection of another region of interest located in ERBS block. This region was selected due to this material's homogeneous density and, consequent, low internal SD (no artifacts).

In general, according to the SD and CNR values, the titanium implant did not produce very remarkable artifacts, except for some areas closer to the implant located 90° in relation to the long axis of the mandible body (ROI 1) in Picasso. Differently, other studies found massive beam-hardening artifacts arise for titanium implants.[9,13,15] The difference between these findings can be attributed to the particularities of each study design, considering that only those areas adjacent or very close to the implant were previously analyzed,[9,13,15] while here we evaluated the intensity of these artifacts in greater distances to the implant.

On the other hand, zirconium implants behaved, in most cases, differently from other groups in all CBCT scanners, presenting higher SD values. Probably, the reason is related to the properties of this material, since the atomic number (Z = 40) is higher than titanium (Z = 22). A tendency for artifacts to decrease with distance from the implant was expected and it was in fact observed. However, it is important to highlight that, although the artifact is more pronounced in the regions closer to the implant, it can reach as far as 3.5 cm from the artifact-generator object, depending on the scanner.

A previous study assessed the gray values at 0.5 mm, 1 mm and 2 mm from the surface of the titanium, titanium-zirconium or zirconium implant.[15] Similar to our study, the authors concluded that the zirconium generated more artifacts than other types of implant, mostly in the regions closer to the implant. However, the furthest distance from the implants evaluated was 2 mm, which is still very close to the object. As explained previously, different from other studies that tested the artifact around the implant and its impact on implant-related diagnoses such as peri-implant fenestration and dehiscence,[22,23] our main goal was to evaluate the artifact production when the implant analysis is not the reason for the CBCT requirement, but it still is in the FOV.

Similar to SD, the CNR values of control and titanium groups of three CBCT units showed they are homogeneous images. Otherwise, the zirconium group behaved in an unusual way for each unit, but in general confirming the reduction of image quality in the regions located at 1–2 cm and 90° in relation to the long axis of the mandible body. Only Picasso Trio and ProMax 3D presented difference between implant types; however, the majority of ROIs showed lower CNR values for the zirconium group, corroborating its negative influence on image quality.

As previously stated, the literature presents a paucity of studies that have evaluated the effect of artifacts produced by high-density materials far from its source. In this sense, there are few previous studies that may be compared with our findings. Considering that we observed different behavior between the types of implants and the CBCT scanners, new studies evaluating the magnitude of artifacts produced by other metallic restorative materials in other machines should be performed. Since the intensity of the artifacts produced in CBCT images was higher in regions closer to the dental implants, further studies are needed to evaluate the interference of artifacts in the diagnosis of pathological conditions adjacent to the implant.

In a clinical context, our results suggest that the presence of dental implants either titanium or mainly zirconium, causes a decrease in the image quality even in distant regions of the site of installation. Consequently, they can affect the evaluation of other areas that are located near or far from the region where the dental implant is, proving that the artifacts are not restricted to the region near to high-density material. Thus, diagnostic capacity in other areas that are located far from the artifact-forming region may be difficult, and clinical investigations are needed to better elucidate this hypothesis.

In addition, some authors observed that adjustments in exposure protocols in different clinical contexts may improve the CBCT image quality.[5,14,18,24] However, it seems there are no data about the impact of changes in exposure protocol on magnitude of artifacts caused by the beam-hardening phenomenon. Thus, we encourage future studies to establish exposure protocols that promote a better relationship between exposure dose and quality in evaluation of CBCT images in regions surrounding implants.

Conclusion

Quantity and magnitude of the artifacts in CBCT images can be influenced by the type of dental implant and CBCT unit. Zirconium implants have greater deleterious effects on image quality. Although they are more pronounced in the regions closer to the implant and located at 90° in relation to the mandibular long axis, they can reach as far as 3.5 cm from the artifact-generating object. In view of spread of the use of CBCT and the importance of its artifacts in the clinical practice of dentistry as well as the variability of the results, the authors encourage the professionals to be aware of how the artifacts may be extensive in their own scanners, if they work with different units than those studied here.

Acknowledgements

This study was partially supported by CAPES (Coordenação do Aperfeiçoamento de Pessoal de Nível Superior-Brazil).

References

1. Tyndall DA, Price JB, Tetradis S, Ganz SD, Hildebolt C, Scarfe WC. Position statement of the American academy of oral and maxillofacial radiology on selection criteria for the use of radiology in dental implantology with emphasis on cone beam computed tomography. *Oral Surg Oral Med Oral Pathol Oral Radiol* 2012; **113**: 817–26. doi: https://doi.org/10.1016/j.oooo.2012.03.005
2. SEDENTEXCT Project. *European commission. Radiation protection Nº. 172 sedentexCT. guidelines on CBCT for Dental and Maxillofacial Radiology*. Luxembourg: EU publications office; 2012.
3. Harris D, Horner K, Gröndahl K, Jacobs R, Helmrot E, Benic GI, et al. E.A.O. guidelines for the use of diagnostic imaging in implant dentistry 2011. a consensus workshop organized by the European association for osseointegration at the medical university of Warsaw. *Clin Oral Implants Res* 2012; **23**: 1243–53. doi: https://doi.org/10.1111/j.1600-0501.2012.02441.x
4. Scarfe WC, Farman AG. What is cone-beam CT and how does it work? *Dent Clin North Am* 2008; **52**: 707–30. doi: https://doi.org/10.1016/j.cden.2008.05.005
5. Vasconcelos TV, Bechara BB, McMahan CA, Freitas DQ, Noujeim M. Evaluation of artifacts generated by zirconium implants in cone-beam computed tomography images. *Oral Surg Oral Med Oral Pathol Oral Radiol* 2017; **123**: 265–72. doi: https://doi.org/10.1016/j.oooo.2016.10.021
6. Machado AH, Fardim KAC, de Souza CF, Sotto-Maior BS, Assis N, Devito KL. Effect of anatomical region on the formation of metal artefacts produced by dental implants in cone beam computed tomographic images. *Dentomaxillofac Radiol* 2018; **47**: 20170281. doi: https://doi.org/10.1259/dmfr.20170281
7. Schulze R, Heil U, Gross D, Bruellmann DD, Dranischnikow E, Schwanecke U, et al. Artefacts in CBCT: a review. *Dentomaxillofac Radiol* 2011; **40**: 265–73. doi: https://doi.org/10.1259/dmfr/30642039
8. Benic GI, Sancho-Puchades M, Jung RE, Deyhle H, Hämmerle CH. In vitro assessment of artifacts induced by titanium dental implants in cone beam computed tomography. *Clin Oral Implants Res* 2013; **24**: 378–83. doi: https://doi.org/10.1111/clr.12048
9. Pauwels R, Stamatakis H, Bosmans H, Bogaerts R, Jacobs R, Horner K, et al. Quantification of metal artifacts on cone beam computed tomography images. *Clin Oral Implants Res* 2013; **24**: 94–9. doi: https://doi.org/10.1111/j.1600-0501.2011.02382.x
10. De Man B, Nuyts J, Dupont P, Marchal G, Suetens P. Metal streak artifacts in X-ray computed tomography: a simulation study. *IEEE Trans Nucl Sci* 1999; **46**: 691–6. doi: https://doi.org/10.1109/23.775600
11. Prell D, Kyriakou Y, Beister M, Kalender WA. A novel forward projection-based metal artifact reduction method for flat-detector computed tomography. *Phys Med Biol* 2009; **54**: 6575–91. doi: https://doi.org/10.1088/0031-9155/54/21/009
12. - Rao GV, Rao SA, Mahalakshmi PM, Soujanya E. Cone beam computed tomography: an insight beyond eyesight in clinical dentistry. *Innov J Med Health Sci* 2012; **2**: 74–80.
13. Schulze RK, Berndt D, d'Hoedt B, d'Hoet B. On cone-beam computed tomography artifacts induced by titanium implants. *Clin Oral Implants Res* 2010; **21**: 100–7. doi: https://doi.org/10.1111/j.1600-0501.2009.01817.x
14. Bechara B, McMahan CA, Moore WS, Noujeim M, Geha H. Contrast-to-noise ratio with different large volumes in a cone-beam computerized tomography machine: An in vitro study. *Oral Surg Oral Med Oral Pathol Oral Radiol* 2012; **114**: 658–65. doi: https://doi.org/10.1016/j.oooo.2012.08.436
15. Sancho-Puchades M, Hämmerle CH, Benic GI. In vitro assessment of artifacts induced by titanium, titanium-zirconium and zirconium dioxide implants in cone-beam computed tomography. *Clin Oral Implants Res* 2015; **26**: 1222–8. doi: https://doi.org/10.1111/clr.12438
16. Omar G, Abdelsalam Z, Hamed W. Quantitative analysis of metallic artifacts caused by dental metallic restorations: comparison between four CBCT scanners. *Future Dental Journal* 2016; **2**: 15–21. doi: https://doi.org/10.1016/j.fdj.2016.04.001
17. Horner K, O'Malley L, Taylor K, Glenny AM. Guidelines for clinical use of CBCT: a review. *Dentomaxillofac Radiol* 2015; **44**: 20140225. doi: https://doi.org/10.1259/dmfr.20140225
18. Bezerra IS, Neves FS, Vasconcelos TV, Ambrosano GM, Freitas DQ. Influence of the artefact reduction algorithm of Picasso Trio CBCT system on the diagnosis of vertical root fractures in teeth with metal posts. *Dentomaxillofac Radiol* 2015; **44**: 20140428. doi: https://doi.org/10.1259/dmfr.20140428
19. Bushberg JT. Eleventh annual Warren K. Sinclair keynote address-science, radiation protection and NCRP: building on the past, looking to the future. *Health Phys* 2015; **108**: 115–23. doi: https://doi.org/10.1097/HP.0000000000000228
20. Oenning AC, Jacobs R, Pauwels R, Stratis A, Hedesiu M, Salmon B.DIMITRA Research Group, http://www.dimitra.be Cone-beam CT in paediatric dentistry: DIMITRA project position statement. *Pediatr Radiol* 2018; **11848**: 4012–9. doi: https://doi.org/10.1007/s00247-017-4012-9
21. Bechara B, McMahan CA, Geha H, Noujeim M. Evaluation of a cone beam CT artefact reduction algorithm. *Dentomaxillofac Radiol* 2012; **41**: 422–8. doi: https://doi.org/10.1259/dmfr/43691321
22. de-Azevedo-Vaz SL, Vasconcelos KF, Neves FS, Melo SL, Campos PS, Haiter-Neto F. Detection of periimplant fenestration and dehiscence with the use of two scan modes and the smallest voxel sizes of a cone-beam computed tomography device. *Oral Surg Oral Med Oral Pathol Oral Radiol* 2013; **115**: 121–7. doi: https://doi.org/10.1016/j.oooo.2012.10.003
23. Kamburoğlu K, Murat S, Kılıç C, Yüksel S, Avsever H, Farman A, et al. Accuracy of CBCT images in the assessment of buccal marginal alveolar peri-implant defects: effect of field of view. *Dentomaxillofac Radiol* 2014; **43**: 20130332. doi: https://doi.org/10.1259/dmfr.20130332
24. Bechara B, Alex McMahan C, Moore WS, Noujeim M, Teixeira FB, Geha H. Cone beam CT scans with and without artefact reduction in root fracture detection of endodontically treated teeth. *Dentomaxillofac Radiol* 2013; **42**: 20120245. doi: https://doi.org/10.1259/dmfr.20120245